Soils and Rocks
An International Journal of Geotechnical and Geoenvironmental Engineering
www.soilsandrocks.com
ISSN 1980-9743
ISSN-e 2675-5475

A parametric study on the stability of tailings storage facilities with cemented berms

Leonardo Ribeiro[1#], Sara Rios[1], Marcos Arroyo[2], Miguel Mánica[3]

Article

Keywords
Limit equilibrium method (MEL)
Slopes
Factor of safety
Mine tailings
Dry stack
Soil stabilization

Abstract
A parametric study using the limit equilibrium method was carried out to evaluate the influence of a berm of cemented tailings on the stability conditions of dry stack tailings storage facilities over different water table configurations. More than 9000 analyses were performed, assuming drained and undrained conditions, examining the effect of variations in the height of the embankment and the width of the reinforcement berm, as well as the strength of the cemented and uncemented tailings materials. Three different configurations of the water table were considered, simulating a normal scenario and the consequences of heavy rainfall or poor drainage. Results provide relevant insights into the factors involved in the stabilization of dry stacked tailings with cemented berms, including a linear relationship between the factor of safety and a normalized berm width. The fitting coefficients of this correlation were also shown to be dependent on uncemented and cemented soil strength parameters. For conditions similar to those considered in this study, these results can be used as a screening tool to obtain initial estimates of berm dimensions and cemented tailings strength.

1. Introduction

The mining industry is crucial for modern society, providing essential minerals for energy transition and digitalization. The supply of mineral raw materials requires adequate management of tailings (the fine material is discarded after ore extraction). Tailings have been traditionally disposed of as hydraulic fills in dams raised by staged construction. However, the safety track record of these structures has been unsatisfactory to date, accumulating a significant number of large-scale failures (e.g., Stava, Italy, 1985; Aznalcollar, Spain, 1998; Mount Polley, Canada, 2014; Fundao, Brazil, 2015; or Brumadinho, Brazil, 2019) with severe consequences (casualties, damages, environmental impacts, and serious disruptions on the supply of mineral raw materials). Most of these major large-scale failures have been related to static liquefaction. Static liquefaction is a consequence of undrained strength brittleness in loose (contractive) saturated deposits, in which undrained shearing goes through a peak before attaining critical state conditions at much lower stresses (Gens, 2019). Hydraulically deposited tailings are loose, difficult to maintain in unsaturated state, and frequently show a brittle undrained response; as a result, they are often susceptible to liquefaction.

As an alternative to hydraulic deposition, dry stacking disposal consists of filtered tailings (with lower water contents) compacted in massive embankments, which can reach heights of more than 100 m. The term "dry stack" is a misnomer (Davies, 2011), as the initial degree of saturation is generally between 70-85%, depending on the filtration process, grain size and type of material, transportation mode, and climate conditions. This solution was traditionally associated with arid climates (Lara Montani et al., 2013) but is currently being considered also in other climates. The benefits of stacked tailings facilities include much reduced stored and processing water volumes and improved geotechnical conditions (Furnell et al., 2022).

Dry stack deposition results in materials that are far denser than those deposited hydraulically, and, as a result, they are not expected to be contractive (Oldecop & Rodari, 2021). However, even if liquefaction susceptibility is unlikely this does not mean that undrained conditions are not relevant. Embankments resulting from dry stack disposal are generally designed with drainage systems, similar to those in tailings dams. However, since these structures, composed of silt-size

#Corresponding author. E-mail address: up201800308@up.pt
[1]Universidade do Porto, Faculdade de Engenharia, CONSTRUCT - GEO, Porto, Portugal.
[2]Universidad Politécnica de Cataluña, Departamento de Ingeniería del Terreno, Barcelona, España.
[3]Universidad Nacional Autónoma de México, Instituto de Ingeniería, Ciudad de México, México.

Submitted on December 11, 2024; Final Acceptance on July 30, 2025; Discussion open until February 31, 2026.
Editor: Renato P. Cunha
https://doi.org/10.28927/SR.2026.009424

materials, are in service for many years, drainage systems may tend to clog or have reduced drainage capacity. Accidents occurring in tailings dams are often related to problems in the drainage system, leading to a rise in the water table that might trigger an undrained failure. Similarly, in a filtered dry stack, where deficient drainage conditions exist, a material placed in a partially saturated state can become later saturated by compaction or due to rainfall infiltration, which may increase during the facility's lifetime as a consequence of climate change. This is especially relevant for tropical climates (Gomes et al., 2019; Norambuena Mardones et al. 2023; Vizcarra et al., 2024). Depending on the permeability and the loading rate (due to subsequent lifts), excess pore pressures can be generated, mobilizing undrained strength ratios. As a result, undrained failure is a possibility that should not be lightly discarded for dry-stack deposits. A robust design will consider that possibility and, for instance, prevent failure by introducing a reinforced berm.

The reinforcement of existing tailings deposits or dry stacks can be done by building external structural zones, or berms, with cemented filtered tailings. This is relevant in the context of the design of new tailings storage facilities (TSF), to remine existing TSFs with accumulated resources, or for remediation and closure plans. Several studies have addressed binder-based tailings improvement: for instance, Consoli et al. (2022) studied the behavior of tailings stabilized with ordinary Portland cement for use in dry stacks; Boschi et al. (2022) examined permeation grouting on the structural zone as a remedial strategy. However, no studies were found that examine systematically the effectiveness of a cemented structural zone to improve the stability of dry-stack TSF.

Stress-deformation hydromechanical simulations of tailings storage facilities are gaining acceptance over traditional limit equilibrium analyses (LEA). However, these advanced analyses have so far mainly been used to identify the causes of a given failure rather than for design purposes (Morgenstern et al., 2015; Jefferies et al., 2019; Arroyo & Gens, 2021; Mánica et al., 2022; Shuttle et al., 2022), as there is still no consensus on design criteria for stress-deformation numerical analysis with advanced constitutive models. For this reason, LEAs are still used in design while more advanced analyses are generally used for verification purposes. Moreover, LEAs are much faster to perform, being ideal for parametric studies.

In this work, a parametric study was performed to assess the effect of a cemented berm on the stability conditions of a dry stack TSF using LEAs. Variations in the height of the embankment and the width of the berm were studied, as well as the strength of the cemented and uncemented tailings materials. Both drained and undrained conditions were considered, as well as three different configurations of the water table that might occur due to heavy rainfall or a poor drainage system. Results are intended to provide a reference guide for preliminary design where reinforcement is required to achieve a certain level of safety (Schnaid et al., 2020).

2. Description of the parametric study

2.1 Model geometry and hydraulic conditions

The model geometry considered for this work is illustrated in Figure 1 and is intended to represent a typical configuration of a dry stack TSF, with the incorporation of a berm of cemented tailings to improve stability conditions. It is assumed that the embankment is constructed on top of firm ground and, therefore, the failure mechanism cannot comprise the foundation layer. The slope angle was fixed at 30º in all analyses, while slope heights H of 30, 35, and 40 meters were considered. The width of the cemented berm W is also assumed to vary from 0 to 25 meters, using 5-meter increments.

Three different configurations of the water table were also considered to represent conditions related to heavy rainfall or an insufficient drainage system; they are depicted in Figure 2. The first (WT1) and second (WT2) configurations assume a water table close to the embankment crest (distances indicated in Figure 2a and 2b are maintained for all embankment heights). WT1 considers

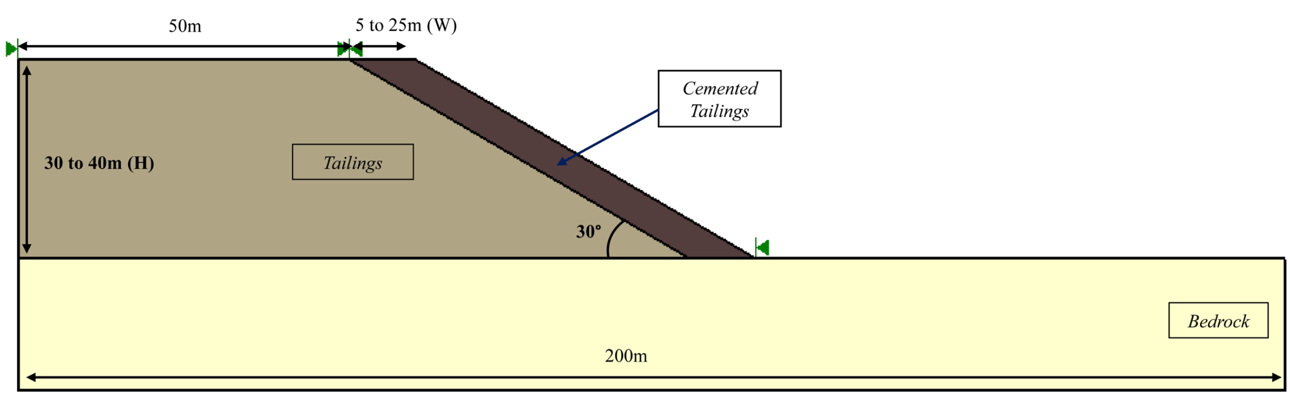

Figure 1. Geometry adopted.

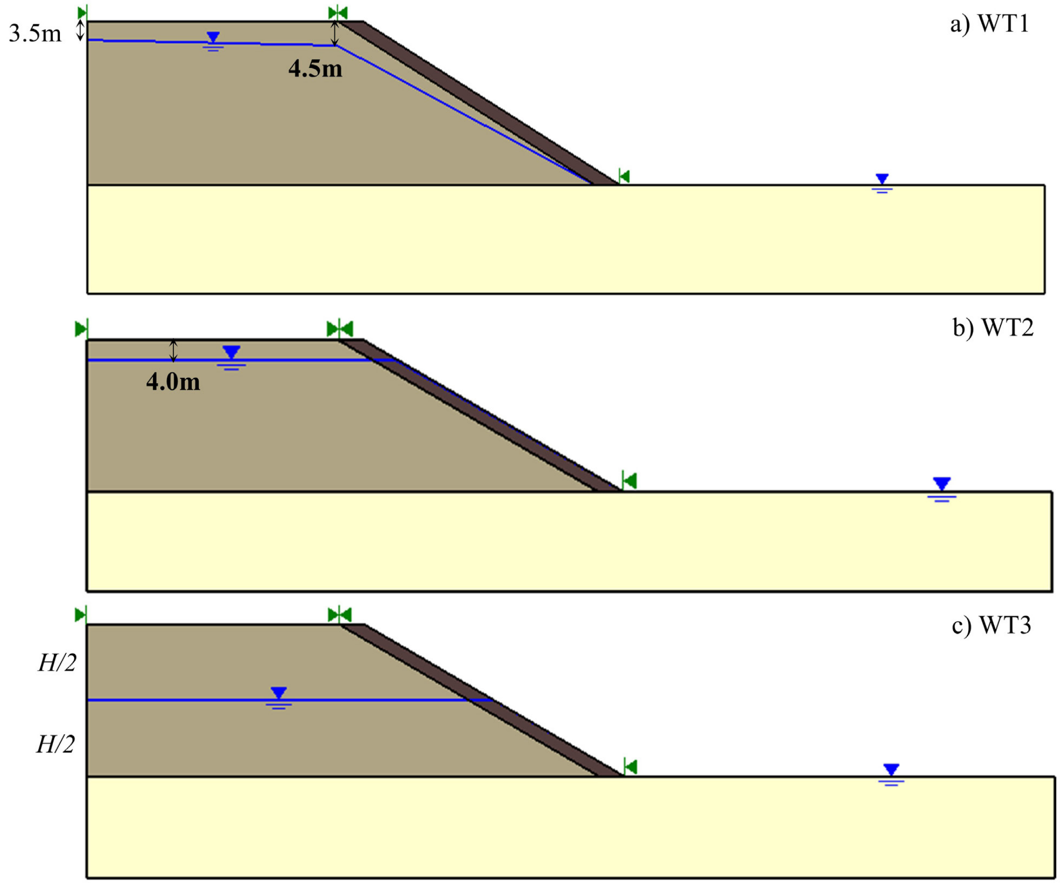

Figure 2. Water table configurations assumed in the analyses: (a) WT1, (b) WT2, and (c) WT3

that some drainage occurs at the embankment toe and, therefore, the cemented berm remains above the phreatic surface. On the other hand, WT2 represents an extreme situation where the drainage system is not working, and the cemented berm remains under the water table. The third configuration (WT3) also assumes poor drainage, but with a water table at mid-height of the embankment, representing a somewhat more moderate wetting scenario. In all cases, it was considered that the soil above the water table was saturated by capillarity, and any effect of suction on the strength was neglected. The schematic water table configurations just described are not the result of seepage analysis and therefore would only approximate real cases, however they define conservative estimates of possible scenarios that are appropriate for screening-level estimates.

2.2 Analyses performed

Several limit equilibrium analyses were performed as part of this parametric study, using the Morgenstern & Price (1965) method, implemented in the software PLAXIS LE v21, to evaluate the stability of slopes reinforced with structural berms made from cemented tailings. As indicated in the flowchart shown in Figure 3, 120 conditions were evaluated in this research. The critical slip surface was defined using the composite circular slip shape, auto refine search method, and slip optimization activated. For each condition (except for those with W = 0), 101 LEAs were performed varying the shear strength of the cemented berm using the sensitivity analysis tool in PLAXIS LE, resulting on about 9100 analyses.

Both drained and undrained conditions were considered. However, drained conditions were only assumed for WT1, since this is the scenario that accounts for active drainage at the embankment toe. Undrained conditions were considered for the three configurations of the water table (WT1, WT2, and WT3), representing extreme cases where the slope becomes saturated due to non-existent or poor drainage. Analyses for this condition were performed to study the berm width and cementation level that may be necessary if the capacity of the drainage system is reduced, and the water table is allowed to rise within the embankment.

2.3 Material properties

Table 1 summarizes the material properties considered for undrained and drained analyses. These properties are partly inspired by laboratory tests results on uncemented and cemented tailings described briefly in Viana da Fonseca et al. (2023).

The drained shear strength of the uncemented tailings was characterized by the Mohr-Coulomb criterion, in terms of friction angle ϕ' and cohesion c'. On the other hand, the undrained shear strength S_u is adopted for undrained analyses (i.e., a Tresca failure criterion). However, the undrained strength for uncemented tailings is assumed to depend on the initial consolidation stress and, therefore, is specified in terms of a given undrained strength ratio S_u / σ'_{v0}. A minimum value of 5 kPa was imposed to prevent null undrained strength values at the crest of the embankment. The undrained strength ratio values considered cover the most usual range of undrained peak strength for tailings materials. As mentioned above, it is hypothesized that dry-stack placement results in materials that are not contractive, and therefore a stability check with undrained residual strength is not necessary.

In the case of the cemented berm, the undrained shear strength is assumed to be mainly related to the effect of the cementing agent; thus, a constant S_u^c was considered. The variation of the strength of the cemented tailings was considered by means of the sensitivity analysis tool in PLAXIS LE, considering an undrained strength S_u^c range between 45 and 500 kPa, determined according to results of unconfined compression tests on cemented tailings from the literature (Consoli et al., 2022; Santos et al., 2022; Servi et al., 2022; Caetano et al., 2023), and assuming that the unconfined compression strength UCS is twice the value of S_u^c.

Regarding the variation of the shear strength of the cemented berm, it is important to mention that the sensitivity analysis tool in PLAXIS LE assumes a fixed slip surface, instead of searching for the critical surface leading to the lowest factor of safety (FS) for a particular strength.

To reduce errors associated with a fixed slip surface when assessing different berm strengths with the sensitivity tool, a reference slip surface for each condition was defined for the mean undrained strength of the cemented tailings, i.e., a value of about 275 kPa. For values in the upper and lower ends of the undrained strength range considered, differences with respect to analyses determined with a critical slip surface search will be larger. These variations were quantified through a series of exploratory analyses, for specific cases, where absolute errors in the FS lower than 0.12 were identified. Errors are low for smaller FSs, reaching values higher than 0.08 only for FSs larger than 1.5.

Table 1. Material properties.

Material	Properties
Uncemented tailings in undrained conditions	S_u / σ'_{v0} = 0.20, 0.23, 0.30 Minimum S_u = 5 kPa γ = 18.1 kN/m³
Uncemented tailings in drained conditions	c' = 2 kPa ϕ' = 33.4° γ = 18.1 kN/m³
Cemented tailings	S_u^c = [45, 500] kPa γ^c = 19 kN/m³

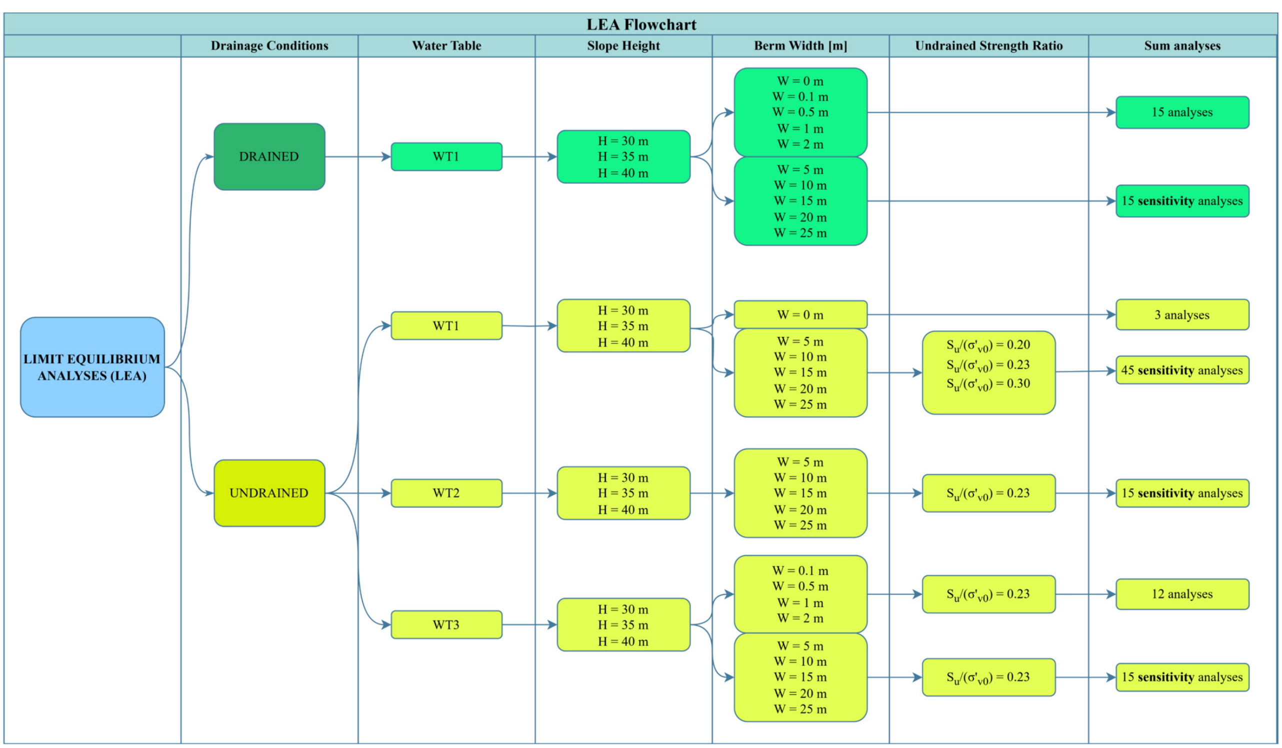

Figure 3. Flowchart of the 120 conditions studied in this work.

Therefore, this simplification has a limited impact on the stability analyses performed.

3. Results

3.1 Slope stability without a cemented berm

Initially, LEAs without the cemented berm ($W = 0$) were performed, for drained and undrained conditions, to serve as a benchmark for subsequent analysis. Figure 4 summarises the results obtained for WT1 only. As expected, since the configuration of the water table represents quite unfavorable conditions, the factors of safety are fairly small, especially for undrained conditions. Table 2 shows the resulting factors of safety for the conditions presented in Figure 4 as well as for the other water table configurations in undrained conditions.

3.2 Slope stability with a cemented berm in drained conditions

In this section, the results of 15 groups of analyses in drained conditions are presented, corresponding to the evaluation of three slope heights (30, 35, and 40 meters), each with five berm widths (5, 10, 15, 20, and 25 meters). As described in Section 2.2, for this drained case only the WT1 configuration was adopted. For each group, 101 LEAs were performed where the *UCS* of the cemented berm varied from 90 to 1000 kPa. However, when the strength of the cemented material is lower than 200 kPa the cemented berm results in a detrimental effect with respect to the case without a berm, a situation that is certainly not desired to occur in practice. Consequently, the data analyzed in this work considered cases with *UCS* values greater than 200 kPa for the cemented berm.

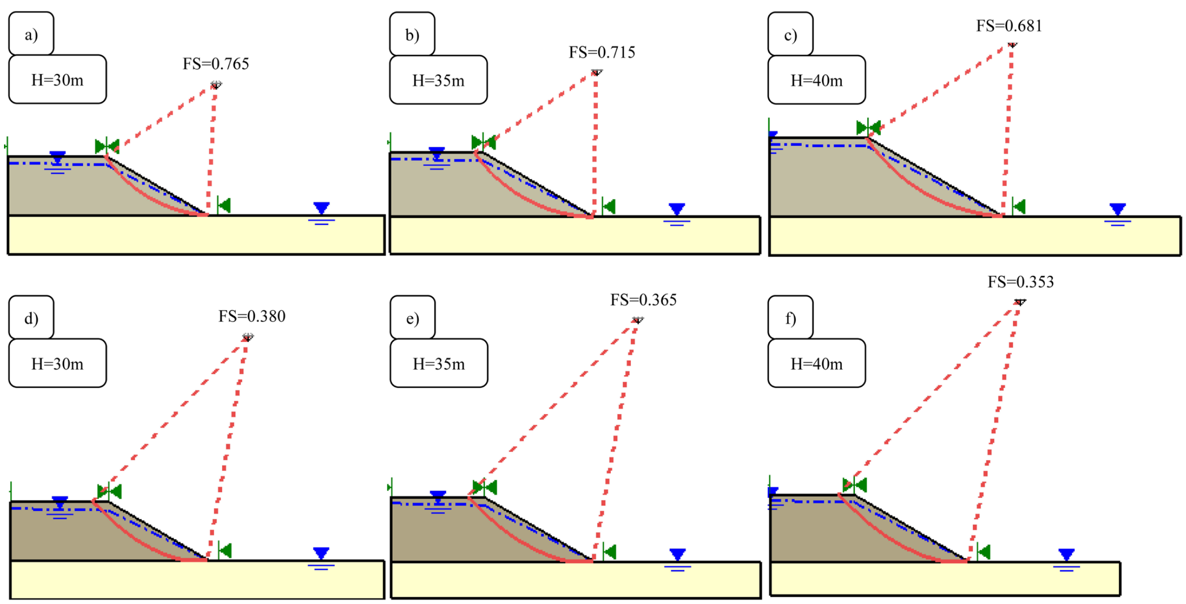

Figure 4. Slip surfaces and *FS*s for different slope heights considering WT1 and drained (a, b, and c) and undrained (d, e, and f) conditions.

Table 2. Factors of safety for models without cemented berm.

Water Table	Condition	Height (m)	Factor of Safety
WT1	Drained	30	0.765
WT1	Drained	35	0.715
WT1	Drained	40	0.681
WT1	Undrained	30	0.380
WT1	Undrained	35	0.365
WT1	Undrained	40	0.353
WT2	Undrained	30	0.271
WT2	Undrained	35	0.265
WT2	Undrained	40	0.263
WT3	Undrained	30	0.366
WT3	Undrained	35	0.361
WT3	Undrained	40	0.358

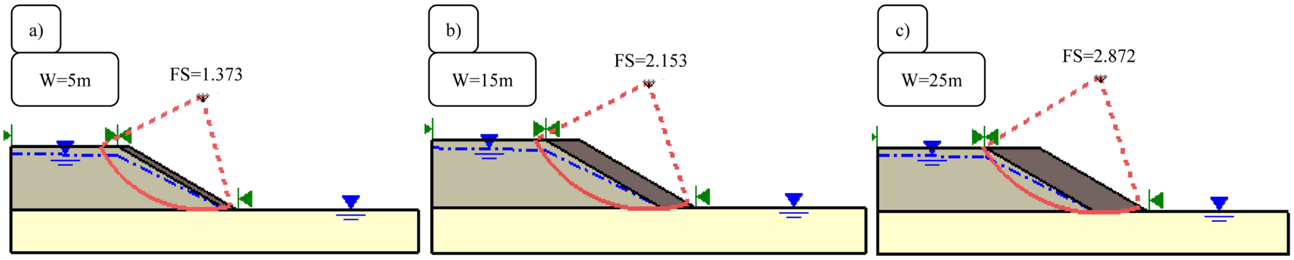

Figure 5. Slip surfaces and factor of safety for a slope height of 30 m, *UCS* of the cemented tailings of 550 kPa in drained conditions and varying berm widths: (a) $W = 5$m, (b) $W = 15$m, and (c) $W = 25$m

Figure 5 shows some examples of the obtained slip surfaces for a slope height of 30 m and a *UCS* value of the cemented berm of 550 kPa. Figure 6a shows the resulting FSs for *UCS* values of 320, 550, 775, and 1000 kPa, while Figure 6b illustrates that a unique trendline is obtained for higher cemented berm strengths. As a way of normalizing the results, FSs are plotted against the nondimensional variable $\overline{W}$, called herein normalized width, defined in Equation 1:

$$\overline{W} = \frac{W\,S_u^c}{H^2\,\gamma} \tag{1}$$

where W is the berm width, H is the slope height, S_u^c is the undrained shear strength of the cemented tailings, and γ is the unit weight of the uncemented tailings. The use of adimensional parameters to summarize the results of slope stability analyses has a long tradition in soil mechanics, going back at least to Taylor (1937). It was found that $\overline{W}$ had a strong correlation with the factor of safety. Other simpler adimensional parameters, such as W / H, were also tested but did not show such a strong correlation with *FS*.

The relationship between *FS* and $\overline{W}$, for different *UCS* values, can be approximated with a linear function, described by the following Equation 2:

$$FS = m\overline{W} + n = m\frac{W\,S_u^c}{H^2\,\gamma} + n \tag{2}$$

where m and n are fitting parameters.

Table 3 shows the parameters m and n corresponding to the trendlines for the *UCS* values shown in Figure 6a. The high correlation coefficients achieved indicate that the height of the embankment has a greater influence on stability conditions than the width of the cemented berm, since $\overline{W}$ is inversely proportional to H^2. The results also show that all factors of safety of the slopes with cemented berms are above 1.0, values that are significantly higher than those obtained from the simulations in Section 3.1 (see Table 2), confirming the effectiveness of the explored range of cemented berms in enhancing stability conditions.

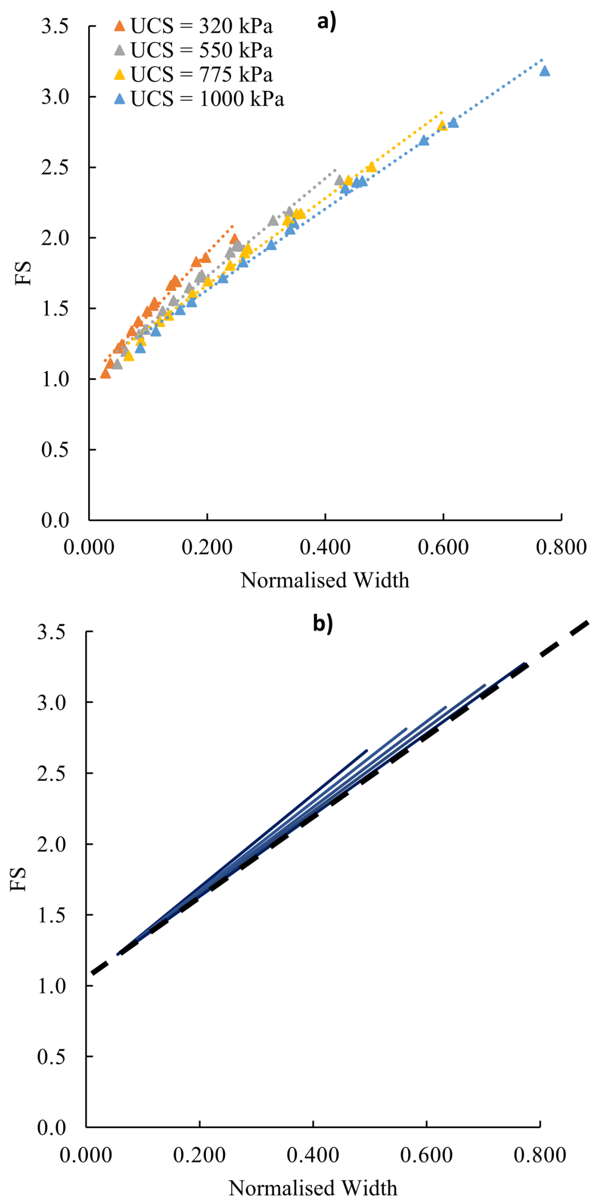

Figure 6. Factors of safety vs. normalized width $\overline{W}$ for drained conditions and WT1: (a) for cemented berms with *UCS* of 320, 550, 775 and 1000 kPa and (b) dashed line representing a unique trendline between *FS* and $\overline{W}$ for higher berm strengths

As expected, increasing the strength of the cemented berm leads to a corresponding increase in the factor of safety. However, as the value of *UCS* increases, the parameter m decreases, meaning that the rate of increase in *FS* as a function of the normalized width $\overline{W}$ is diminished. However, as shown in Figure 7, which illustrates the evolution of the parameters m and n as a function of *UCS* of the cemented tailings, the reduction of m slows down and appears to converge to a certain value. Conversely, the parameter n increases with cementation, but shows a limited variation, with differences of less than 6% across the assumed range of *UCS* values.

Since n corresponds to the y-intercept of a linear function (Equation 2) for $\overline{W} = 0$, it should represent the *FS* for the slope without any reinforcement. However, the *FS* values for the unreinforced slopes, presented in Section 3.1, are significantly lower than those predicted by the trendlines in Figure 6. This suggests that the observed linear trend does not hold for small $\overline{W}$ values. To corroborate this, additional analyses were performed for a wider range of berm widths, from 0.1 m to 25 m, using a single *UCS* value of 550 kPa; the results are shown in Figure 8 together with a linear trendline (see fitting parameters in Table 3). Figure 8a shows all the results while Figure 8b shows a zoom of the results with lower values of $\overline{W}$.

It can be identified that Equation 2, in terms of the normalized width, can adequately describe the behavior of the *FS* for $\overline{W}$ values in the range of about 0.1 to 0.8. Then, as expected, for smaller values, the *FS* shows a marked nonlinear reduction until converging to the case of the slope without a berm. Nevertheless, since the incorporation of a berm is usually intended to significantly improve stability conditions, this nonlinear behavior for low $\overline{W}$ values is not particularly relevant from a practical standpoint. Therefore, the interpretation in terms of Equation 2 is considered adequate.

3.3 Slope stability with a cemented berm in undrained conditions

3.3.1 Effect of the cemented tailings (berm) strength

In this section, the results of 45 groups of analyses in undrained conditions are presented (see Figure 3); 15 for each water table configuration. For each group, 101 LEAs were performed, where the *UCS* of the cemented berm varied from 90 kPa to 1000 kPa, corresponding to the undrained strengths assumed between 45 and 500 kPa (see Table 1). In these cases, 90 kPa was identified in preliminary parametric studies as the lower limit for the *UCS* of the cemented berm that prevents a detrimental effect of the berm on overall stability. In all the analyses described in this section, a fixed undrained strength ratio $S_u / \sigma'_{v0} = 0.23$ was adopted for the uncemented tailings.

Figure 9 shows typical slip surfaces obtained for a slope height of 30 m and a *UCS* value of the cemented berm of 550 kPa, for the three different water table configurations.

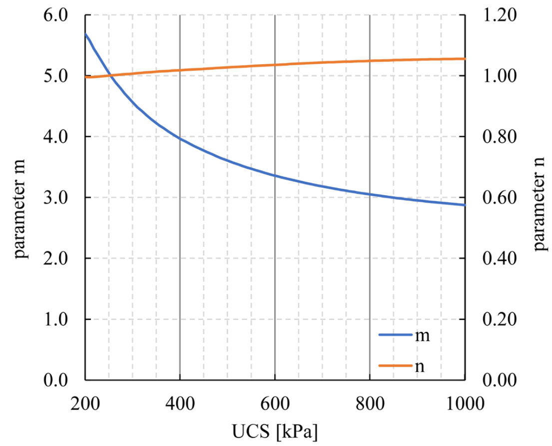

Figure 7. Evolution of fitting parameters m and n as a function of the *UCS* of the cemented berm for drained conditions and WT1.

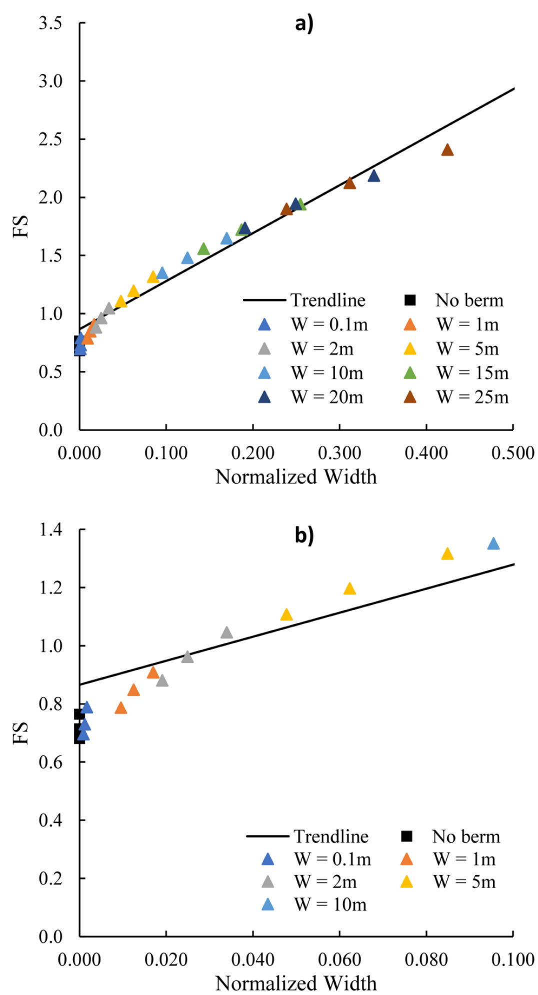

Figure 8. Factor of safety vs. normalized width $\overline{W}$ for drained conditions, WT1, a *UCS* value of 550 kPa, and varying berm widths. The linear trendline has the fitting parameters from Table 3. (a) shows all the results, while (b) shows a zoom in the lower values of the normalized width.

It can be observed that, for the cases studied, the critical surfaces are quite similar for the different water table configurations. Nevertheless, the berm width influences the failure mechanism. For small widths, a near-circular failure surface is observed. However, for larger berms, the failure mechanism involves an arc segment in the lower part, near the toe, and a straight line running approximately parallel to the slope face, at a certain distance from the cemented berm.

Table 3. Fitting parameters in Equation 2 determined for drained conditions and WT1, and for different *UCS* values of the cemented berm.

UCS	*m*	*n*	R^2
320 kPa	4.4144	1.0097	0.9702
550 kPa	3.4712	1.0318	0.9849
775 kPa	3.0798	1.0452	0.9902
1000 kPa	2.8742	1.0557	0.9943

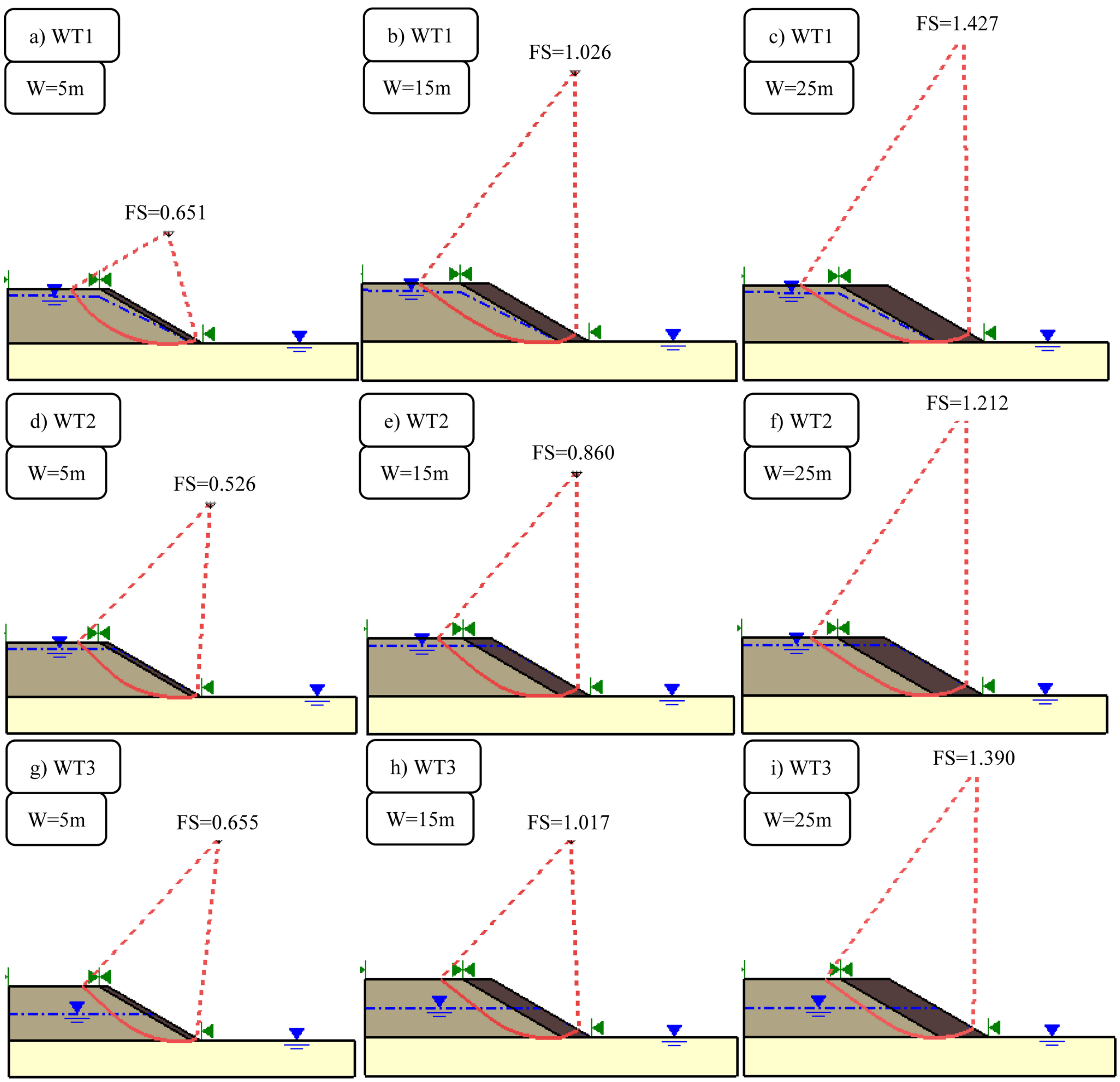

Figure 9. Slip surfaces for a height of 30 m for different water tables and cemented berm widths: (a) WT1 and *W* = 5m, (b) WT1 and *W* = 15m, (c) WT1 and *W* = 25m, (d) WT2 and *W* = 5m, (e) WT2 and *W* = 15m, (f) WT2 and *W* = 25m, (g) WT3 and *W* = 5m, (h) WT3 and *W* = 15m, and (i) WT3 and *W* = 25m,

Figures 10a, 10b and 10c show the factors of safety for the water tables WT1, WT2, and WT3, respectively, and for three selected *UCS* values. Similar to the results in Section 3.2 (Figure 6), as the strength of the cemented berm increases, the corresponding factors of safety also increase, following an approximately linear relationship with respect to $\overline{W}$. Nevertheless, a smaller variation is observed here with respect to the *UCS* values of the cemented tailings and, for each case, the results approximately cluster onto a single line, except for the case with WT1 and *UCS* = 90 kPa, where a certain divergence is observed.

As expected, the FSs for undrained conditions are significantly lower than those for drained conditions. Figure 10d compares the variation of *FS* across the different water table configurations and a constant *UCS* value of 1000 kPa. It is evident that WT2 is the most unfavorable situation, as it corresponds to the case where the water table is closest to the surface and comprises the cemented berm. In contrast, similar results are obtained with WT1 and WT3. Although the water table is higher in WT1, it does not encompass the cemented berm, leading to similar FSs for $\overline{W}$ values greater than 0.4. For smaller $\overline{W}$ values, WT1 produces slightly lower FSs.

Table 4 shows the parameters for Equation 2 corresponding to the trendlines shown in Figure 10, for different UCSs and different configurations of the water table. Again, a strong correlation between $\overline{W}$ and the *FS* can be identified, with R^2 values very close to 1.0. For both drained (Table 3) and undrained (Table 4) conditions, R^2 tends to increase with the strength of the cemented tailings since, as cementation increases, stability conditions become controlled mainly by the berm rather than by the uncemented tailings. The evolution of the fitting parameters is shown in Figure 11.

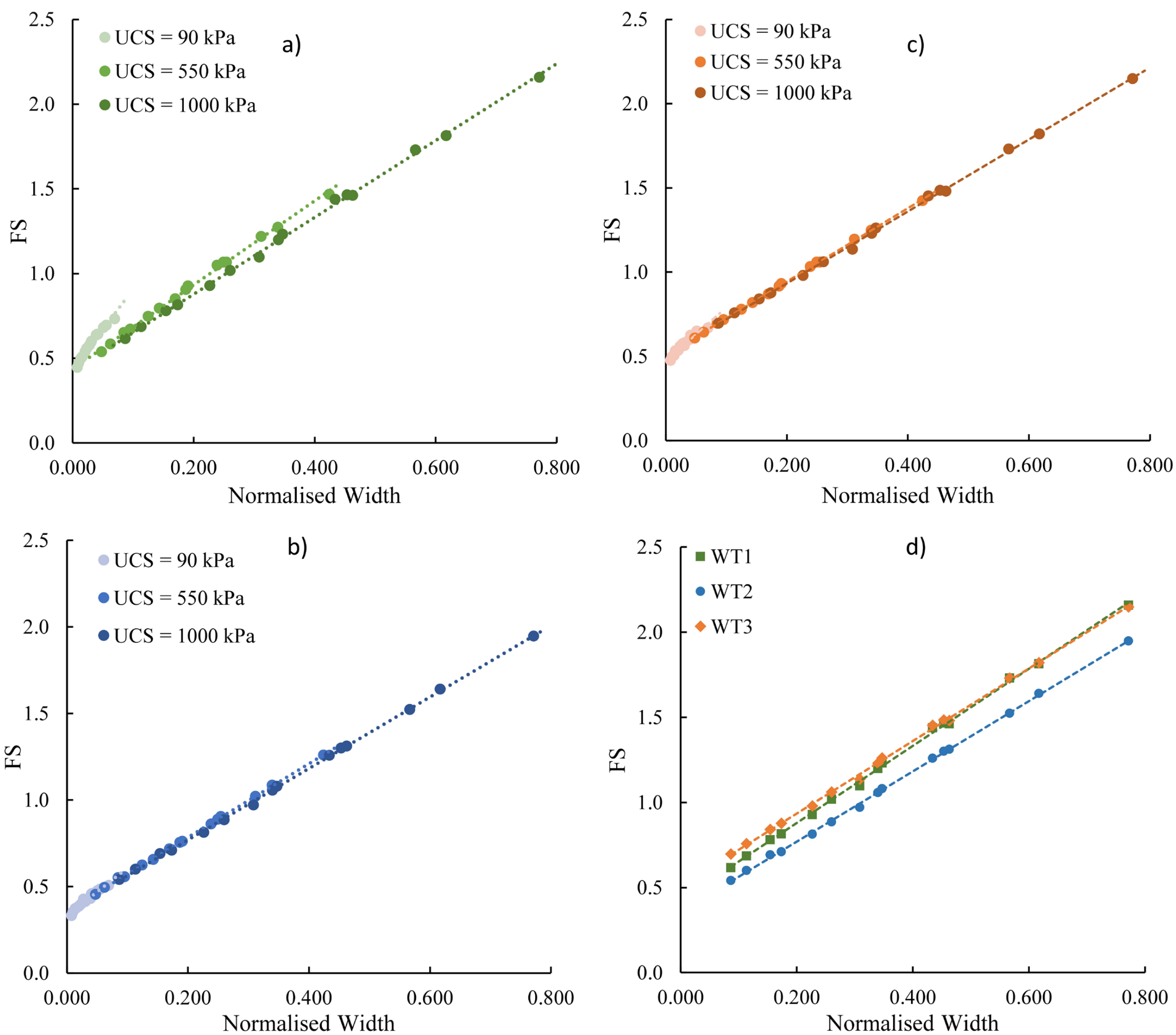

Figure 10. Factor of safety vs. normalized width $\overline{W}$ for undrained conditions, *UCS* values of 90, 500 and 1000 kPa, and water conditions (a) WT1, (b) WT2, and (c) WT3, and (d) for a constant *UCS* value of 1000 kPa and the three water table configurations considered.

Table 4. Fitting parameters in Equation 2 determined for undrained conditions, different water table configurations (WT1, WT2, and WT3), and for different *UCS* values of the cemented berm.

Water table	*UCS* [kPa]	*m*	*n*	R^2
WT1	90	4.7102	0.4374	0.9677
WT1	550	2.4801	0.4372	0.9982
WT1	1000	2.2664	0.4253	0.9988
WT2	90	2.7734	0.3305	0.9552
WT2	550	2.1275	0.3580	0.9995
WT2	1000	2.0633	0.3568	0.9994
WT3	90	3.1880	0.4726	0.9454
WT3	550	2.1779	0.5081	0.9995
WT3	1000	2.1333	0.5070	0.9991

Similar to Figure 7, the *m* parameter tends to decrease as the value of *UCS* of the cemented tailings increases for all water table configurations, while variations in *n* across the whole range of *UCS* values are relatively small (less than 8%). On the other hand, significant variations in *n* can be identified among the different water table configurations, controlling the vertical position of the trendlines (Figure 10d) and reflecting the importance of drainage for stability conditions. The lowest *n* values occur for WT2, corresponding to a situation with poor drainage and a very high water table (Figure 2b). It was also noted that, as the cemented strength increases, the position of the water table has less influence on the *m* parameter. This is because the strength of the cemented tailings is assumed to be stress-independent and, therefore, variations in the effective stress state due to the distribution of water pressures have less impact of stability as the contribution of the cemented berm increases.

As with the drained analyses, the observed linear trend, defined with the parameters from Table 3, does not appear to converge to the *FS*s of the slopes without berms as $\overline{W}$ is reduced. As identified in Figure 12, which shows the variation of the *FS* of additional analyses including low *W* values (for WT3 and *UCS* = 550 kPa), the linear trend does not hold when the berm is less than 2 meters wide. However, as previously mentioned, these cases are not particularly relevant from a practical standpoint.

3.3.2 Effect of the uncemented tailings strength

An additional group of analyses was performed to assess the influence of undrained shear strength of the uncemented tailings on stability conditions. While results in the previous section considered an undrained strength ratio $S_u / \sigma'_{v0} = 0.23$, further analyses were conducted using values ranging from 0.20 to 0.30, which represents the typical range observed in undrained triaxial tests on reconstituted tailings samples (Viana da Fonseca et al., 2022). Figures 13a, 13b and 13c present the results for WT1, WT2, and WT3, respectively, in terms of FSs vs. $\overline{W}$, for the undrained strength ratios of 0.20, 0.23, and 0.30. The fitting parameters of the adjusted trendlines are reported

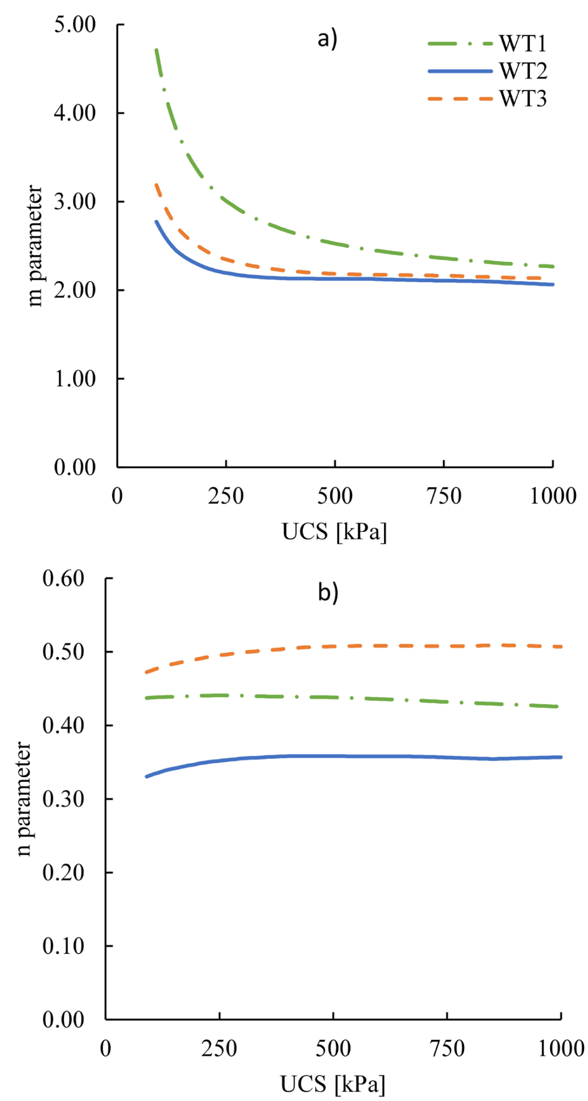

Figure 11. Evolution of the fitting parameters (a) *m* and (b) *n* as a function of the *UCS* of the cemented berm for undrained conditions and the different water table configurations considered.

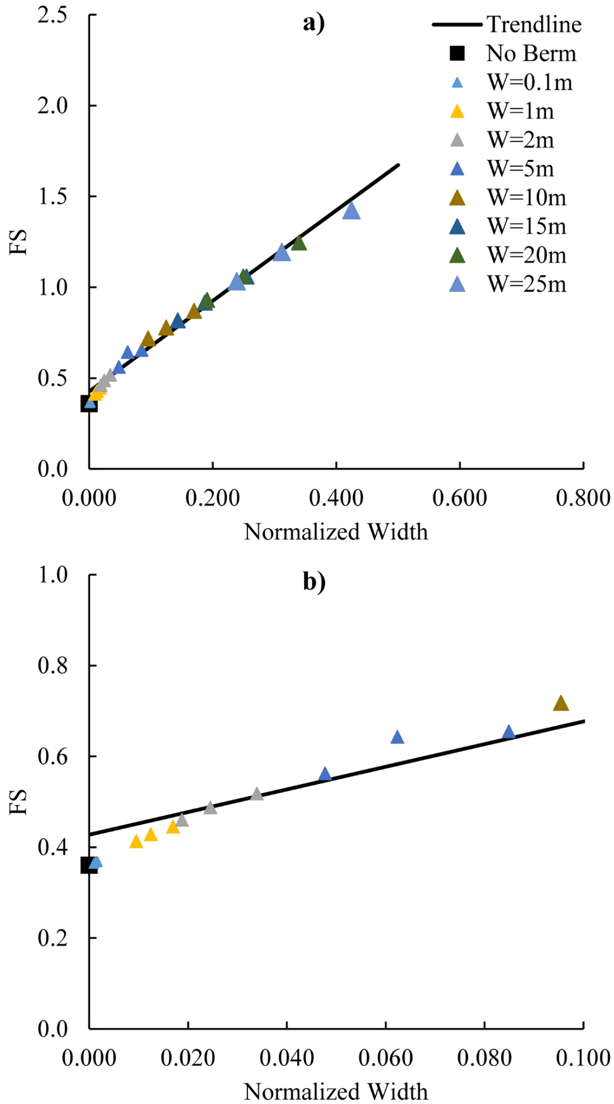

Figure 12. Factor of safety vs. normalized width $\overline{W}$ for undrained conditions, WT3, a *UCS* value of 550 kPa, and varying berm widths. (a) shows all the results, while (b) shows a zoom in the lower values of the normalized width.

in Table 5. Results are presented only for a *UCS* of 550 kPa for the cemented tailings, although they are representative of the behavior observed for other *UCS* values.

It can be identified that the strength of the uncemented tailings does not significantly affect the slope of the trendlines; they are only shifted vertically. Consequently, the parameter *n* varies for different strength ratios, in an approximately linear fashion since this parameter is related to the *FS* for the unreinforced slope. The evolution of the *m* and *n* parameters with varying undrained strength ratio of the uncemented material is displayed in Figure 14.

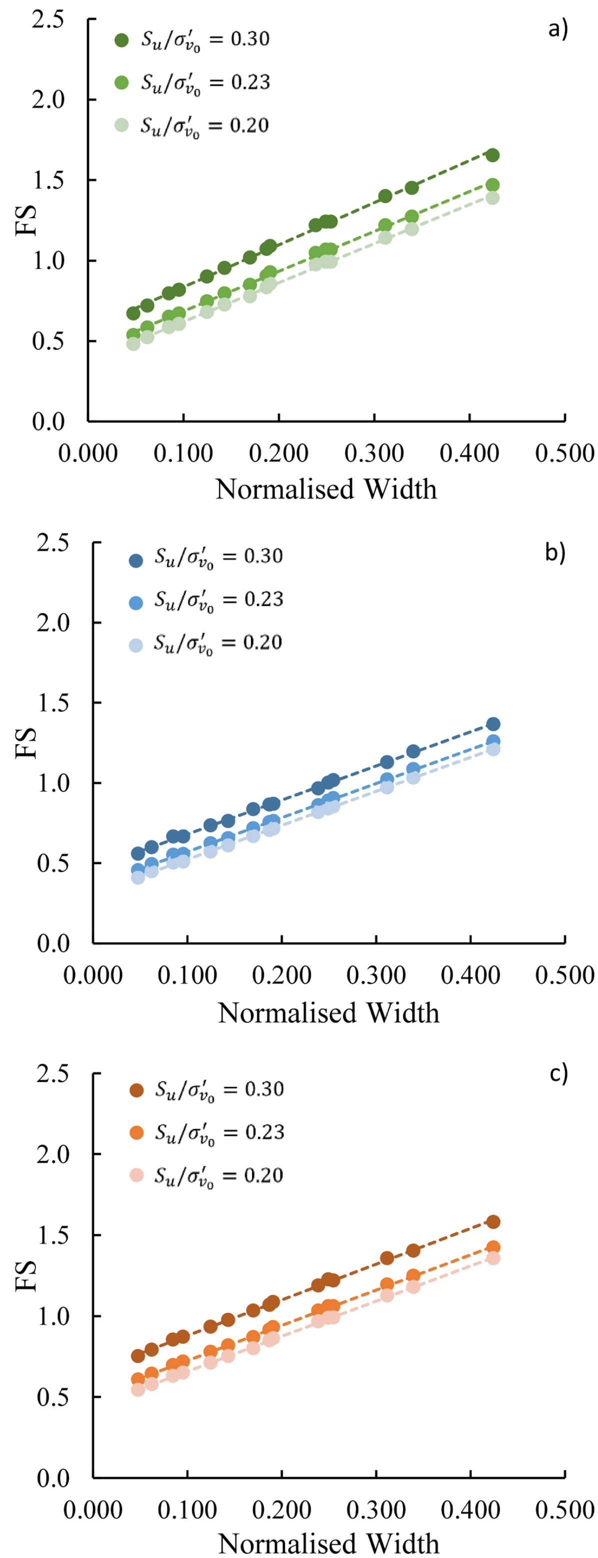

Figure 13. Resulting *FS*s for different configurations, a cemented berm with a *UCS* of 550 kPa, undrained strengths ratios of the uncemented tailings of 0.20, 0.23, and 0.30, and water tables (a) WT1, (b) WT2, and (c) WT3.

Table 5. Fitting parameters in Equation 2 determined for undrained conditions, different water table configurations (WT1, WT2, and WT3), a *UCS* of the cemented tailings of 550 kPa, and for different undrained strength ratios of the uncemented tailings.

Water table	$\frac{S_u}{\sigma'_{v0}}$	m	n	R^2
WT1	0.20	2.4223	0.3785	0.9985
WT1	0.23	2.4801	0.4372	0.9982
WT1	0.30	2.6213	0.5723	0.9972
WT2	0.20	2.1189	0.3115	0.9996
WT2	0.23	2.1275	0.3580	0.9995
WT2	0.30	2.1294	0.4671	0.9988
WT3	0.20	2.1710	0.4422	0.9996
WT3	0.23	2.1779	0.5081	0.9995
WT3	0.30	2.2054	0.6590	0.9989

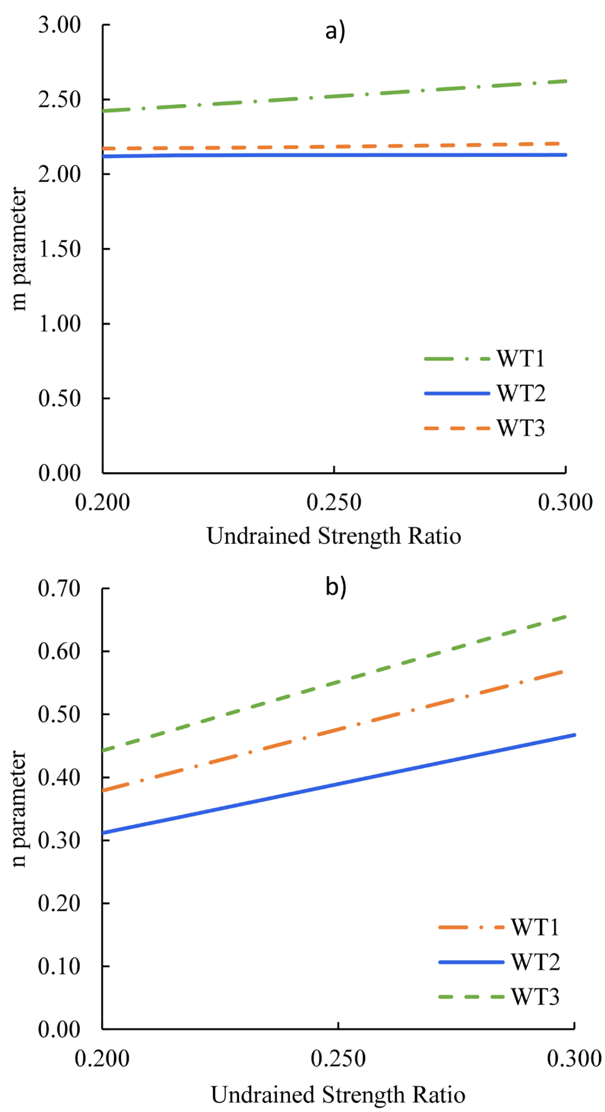

Figure 14. Evolution of the fitting parameters (a) m and (b) n as a function of the undrained strength ratio of the uncemented tailings for undrained conditions and the different water table configurations considered.

4. Conclusion

The limit equilibrium method was employed to perform a parametric study evaluating the influence of a cemented berm on improving stability conditions for dry stack tailings storage facilities. Both drained and undrained parameters for the tailings were considered, as well as different configurations of the water table and strengths of the cemented and uncemented tailings materials. For simplicity three schematic water table configurations were employed, to approximately represent relevant scenarios, without the added complexity of seepage analyses.

Results were assessed in terms of factors of safety as a function of the normalized berm width $\overline{W}$. This latter variable was found to have a strong correlation with *FS*, particularly for higher berm strengths, implying that the height of the slope is significantly more important for stability conditions than the dimensions of the berm, since $\overline{W}$ is directly proportional to W but inversely proportional to the squared of H.

The relationship between *FS* and $\overline{W}$ can be described by means of a linear function, i.e., with a slope m and an intercept n; the first one represents the effect of the cemented berm while the second is related to the *FS* for the unreinforced slope. However, n is not directly equal to the latter since the linear relationship between *FS* and $\overline{W}$ does not hold for small berm widths, which in any case are not of interest from a practical standpoint.

Using this relationship, estimations for minimum widths of the cemented berm to achieve a reasonable safety margin, i.e., *FS* = 1.5, can be made. For example, considering a 30 m high slope in drained conditions, the minimum width of a cemented berm with a *UCS* value of 1000 kPa is estimated at 5.05 m, while, in undrained conditions, it would require at least 15.45m.

The importance of drainage in the stability conditions was demonstrated. The most unfavorable condition was found to be when the water table is close to the crest and over the berm, a situation that should be prevented with an efficient drainage system. However, the different water table configurations have a limited influence on the effect of the cemented berm, i.e., on the parameter m, and changes in the water table mainly shifted the trendlines vertically. Therefore, they are related to the strength of the unreinforced slope. A similar conclusion can be made regarding the undrained strength ratio of the uncemented tailings.

In general, the results obtained provide relevant insights into the factors involved in the stabilization of dry stacked tailings with a cemented berm. For conditions similar to those studied here, results can be directly employed as a screening tool to derive a first estimate of the dimensions of the berm and the required strength of the cemented tailings. The results from such initial estimates may be then refined, for instance by performing seepage analyses appropriate to the case under study or by carrying out stress-deformation analyses.

Acknowledgements

This work was financially supported by national funds through the FCT/MCTES (PIDDAC), namely the CONSTRUCT - Instituto de I&D em Estruturas e Construções, Funding UID/04708, the research project INPROVE-2022.02638. PTDC (https://doi.org/10.54499/2022.02638.PTDC), and by the scholarships of the first author (2024.02301.BDANA) and the second author (CEECIND/04583/2017) (https://doi.org/10.54499/CEECIND/04583/2017/CP1399/CT0003).

Declaration of interest

The authors have no conflicts of interest to declare. All co-authors have observed and affirmed the contents of the paper and there is no financial interest to report.

Authors' contributions

Leonardo Ribeiro: formal analysis, data curation, visualization, writing – original draft. Sara Rios: conceptualization, methodology, supervision, writing – review & editing, funding acquisition, project administration, resources. Marcos Arroyo: validation, investigation, methodology, writing – review & editing. Miguel Mánica: validation, investigation, methodology, writing – review & editing.

Data availability

The datasets generated and analyzed during the current study are included in this article.

Declaration of use of generative artificial intelligence

This work was prepared without the assistance of any generative artificial intelligence (GenAI) tools or services. All aspects of the manuscript were developed solely by the authors, who take full responsibility for the content of this publication.

List of symbols and abbreviations

c'	cohesion
m	Slope of the linear relationship between the FS and $\overline{W}$
n	Intercept of the linear relationship between the FS and $\overline{W}$
A_1	Fitting parameter for the power function relating $\overline{W}$ and undrained strength ratio
A_2	Fitting parameter for the power function relating $\overline{W}$ and undrained strength ratio
FS	Factor of safety
H	Height of the slope
LEA	Limit Equilibrium Analyses
R^2	Coefficient of determination between dependent and independent variables
S_u	Undrained strength of the uncemented tailings
S_u^c	Undrained strength of the cemented tailings
TSF	Tailings Storage Facilities
UCS	Unconfined Compression Strength
W	Width of the cemented berm
$\overline{W}$	Normalized width of the cemented berm
WT	Water Table
γ	Unit weight of uncemented tailings
γ^c,	Unit weight of cemented tailings
σ_{v0}	Initial vertical effective stress
ϕ'	Friction angle

References

Arroyo, M., & Gens, A. (2021). *Computational analyses of Dam I failure at the Corrego de Feijao mine in Brumadinho. Final report from CIMNE to Vale S.A.* Brasília: Ministério Público Federal. Retrieved in December 11, 2024, from http://www.mpf.mp.br/mg/sala-de-imprensa/noticias-mg/desastre-da-vale-relatorio-elaborado-por-universidade-da-espanha-aponta-causas-do-rompimento-da-barragem-em-brumadinho-mg

Boschi, K., Arroyo, M., Burbano, D.A., & Spagnoli, G. (2022). Permeation grouting of an upstream tailing dam: a feasibility study. In *Proceedings of the 26th International Conference on Tailings and Mine Waste* (pp. 59-70), Vancouver, BC. University of British Columbia.

Caetano, I., Rios, S., Viana da Fonseca, A., & Delgado, B. (2023). Stabilization of iron tailings with alkali activated binders. In *Proceedings of the 1st International Conference on Geotechnics of Tailings and Mine Waste* (pp. 127-136), Ouro Preto, MG. ISSMGE.

Consoli, N., Vogt, J., Silva, J., Chaves, H., Scheuermann Filho, H., Moreira, E., & Lotero, A. (2022). Behaviour of compacted filtered iron ore tailings–Portland cement blends: new Brazilian trend for tailings disposal by stacking. *Applied Sciences*, 12(2), 836. http://doi.org/10.3390/app12020836.

Davies, M. (2011). Filtered dry stacked tailings: the fundamentals. In *Proceedings of the 15th International Conference on Tailings and Mine Waste*, Vancouver, BC. University of British Columbia. http://doi.org/10.14288/1.0107683.

Furnell, E., Bilaniuk, K., Goldbaum, M., Shoaib, M., Wani, O., Tian, X., Chen, Z., Boucher, B., & Bobicki, E. (2022). Dewatered and stacked mine tailings: a review. *ACS ES&T Engineering*, 2(5), 728-745. http://doi.org/10.1021/acsestengg.1c00480.

Gens, A. (2019). Hydraulic fills with special focus on liquefaction. In *Proceedings* of the XVII European Conference on Soil Mechanics and Geotechnical Engineering (pp. 52-82). Icelandic Geotechnical Society. Retrieved in December 11, 2024, from https://www.ecsmge-2019.com/uploads/2/1/7/9/21790806/k3-1114-ecsmge-2019_gens_keynote_paper.pdf

Gomes, M.F.M., Mata, J.G., Pinheiro, J.A., & Crystal, C. (2019). Disposal of tailings and the mining industry perspective: a case study of the Cuiabá Mine. In *Proceedings of the 22nd International Conference on Paste, Thickened and Filtered Tailings* (pp. 219-231). Perth: Australian Centre for Geomechanics. http://doi.org/10.36487/ACG_rep/1910_14_Gomes.

Jefferies, M., Morgenstern, N., van Zyl, D., & Wates, J. (2019). *Report on NTSF embankment failure: technical report.* South Orange, NSW: Valley Operations for Ashurst Operations.

Lara Montani, J., Pornillos, E., & Munoz, H. (2013). Geotechnical-geochemical and operational considerations for the application of dry stacking tailings deposits: state-of-the-art. In *Proceedings of the 16th International Seminar on Paste and Thickened Tailings* (pp. 249-260). Crawley, WA: Australian Centre for Geomechanics. http://doi.org/10.36487/ACG_rep/1363_19_Munoz.

Mánica, M., Arroyo, M., Gens, A., & Monforte, L. (2022). Application of a critical state model to the Merriespruit tailings dam failure. *Proceedings of the Institution of Civil Engineers - Geotechnical Engineering*, 175(2), 151-165. http://doi.org/10.1680/jgeen.21.00001.

Morgenstern, N., & Price, V. (1965). The analysis of the stability of general slip surfaces. *Geotechnique*, 15(1), 79-93. http://doi.org/10.1680/geot.1965.15.1.79.

Morgenstern, N., Vick, S., Viotti, C., & Watts, B. (2015). Fundão tailings dam review panel: report on the immediate causes of the failure of Fundao dam. *Blog do Pedlowski. Retrieved in September 29, 2021*, from https://pedlowski.files.wordpress.com/2016/08/fundao-finalreport.pdf

Norambuena Mardones, R.E., Caldwell-Crystal, C., & Cobos Roa, D. (2023). How high is too high? Challenges on the next generation of dewatered tailings stacks. In *Proceedings of the 25th International Conference on Paste, Thickened and Filtered Tailings* (pp. 465-479). Edmonton: University of Alberta. http://doi.org/10.36487/ACG_repo/2355_35.

Oldecop, L., & Rodari, G. (2021). Unsaturated mine tailings disposal. *Soils and Rocks*, 44(3), 135-146. http://doi.org/10.28927/SR.2021.067421.

Santos, C., Bruschi, G., Mattos, J., & Consoli, N. (2022). Stabilization of gold mining tailings with alkali-activated carbide lime and sugarcane bagasse ash. *Transportation Geotechnics*, 32, 100704. http://doi.org/10.1016/j.trgeo.2021.100704.

Schnaid, F., Mello, L., & Dzialoszynski, B. (2020). Guidelines and recommendations on minimum factors of safety for slope stability of tailings dams. *Soils and Rocks*, 43(3), 369-395. http://doi.org/10.28927/SR.433369.

Servi, S., Lotero, A., Silva, J., Bastos, C., & Consoli, N. (2022). Mechanical response of filtered and compacted iron ore tailings with different cementing agents: focus on tailings-binder mixtures disposal by stacking. *Construction & Building Materials*, 349, 128770. http://doi.org/10.1016/j.conbuildmat.2022.128770.

Shuttle, D., Marinelli, F., Brasile, S., & Jefferies, M. (2022). Validation of computational liquefaction for tailings: Tar Island slump. *Geotechnical Research*, 9(1), 32-55. http://doi.org/10.1680/jgere.21.00007.

Taylor, D. (1937). Stability of earth slopes. *Boston Society of Civil Engineering*, 24, 197-246. http://doi.org/10.4236/blr.2012.34026.

Viana da Fonseca, A., Caetano, I., Meneses, B., & Rios, S. (2023). Tailing storage facilities with cemented berms for sustainable production of raw materials. In *Proceedings of the 5th International Conference on Geotechnics for Sustainable Infrastructure Development - GEOTEC HANOI 2023*, Hanoi, Vietnam. London: ISSMGE.

Viana da Fonseca, A., Cordeiro, D., Molina-Gómez, F., Besenzon, D., Fonseca, A., & Ferreira, C. (2022). The mechanics of iron tailings from laboratory tests on reconstituted samples collected in post-mortem Dam I in Brumadinho. *Soils and Rocks*, 45(2), 1-20. http://doi.org/10.28927/SR.2022.001122.

Vizcarra, G., Tehrani, K., Sgavioli, F., Gonçalves, T.M., & Pereira, F. (2024). Key parameters that influence the operation of tailings dry stack disposal considering various international practices. In *Proceedings of the Tailings and Mine Waste Conference*, Denver, CO. USA. Colorado School of Mines.